

# Distance-Based Formation Maneuvering of Non-Holonomic Wheeled Mobile Robot Multi-Agent System

Pablo Hernández-León\* Jorge Dávila\*\* Sergio Salazar\*\*\*  
Xubin Ping\*\*\*\*

\* UMI-LAFMIA, CINVESTAV, Mexico City, Mexico (e-mail:  
pablo.hernandez@cinvestav.mx).

\*\* ESIME-UPT, Instituto Politécnico Nacional, Mexico City, Mexico  
(e-mail: jadavila@ipn.mx)

\*\*\* UMI-LAFMIA, CINVESTAV, Mexico City, Mexico (e-mail:  
sergio.salazar.cruz@gmail.com)

\*\*\*\* Department of Automation, School of Electro-Mechanical  
Engineering, Xidian University, Xi'an, 710075, China (e-mail:  
pingxubin@126.com)

---

**Abstract:** In this paper, finite-time distance-based formation maneuvering control of a non-holonomic wheeled mobile robot multi-agent system in a leader-follower configuration is considered. The desired formation graph is assumed to be minimally and infinitesimally rigid, and only a subset of agents has access to the relative position and velocity of the leader. A distributed velocity estimator is employed by each agent to estimate the leader's velocity and therefore the swarm velocity in finite-time. A finite-time formation maneuvering algorithm is presented and it is proved that drives the agents to the desired formation and tracks the leader's velocity in finite-time. Moreover, it is demonstrated that both the velocity estimator and the controller can be implemented in the agents' local coordinate frames. Simulations are provided to illustrate the effectiveness of the proposed algorithms.

*Keywords:* Multi-agent systems, Coordination of multiple vehicle systems, Distance-based control, Formation maneuvering, Non-holonomic mobile robots.

---

## 1. INTRODUCTION

Decentralized control of multi-agent systems (MAS) has received significant attention due to their practical potential in many civilian and military tasks. An important goal of these systems is formation maneuvering which involves simultaneous shape acquisition and tracking of a reference path or velocity, these objectives allow to achieve practical tasks, see Mehdifar et al. (2018). In Oh et al. (2015) distance-based formation control is presented, where formation is achieved by each agent by sensing the relative positions of its neighbors with respect to their own local coordinate frame through on-board sensors and controlling interagent distances. This strategy compared with position-based and displacement-based control provides more flexibility in the agent implementation, as global information is not required, useful in environments where systems like Global Positioning System (GPS) are not available. Hence by this approach is possible to relax some requirements for multi-agent formation maneuvering or to make full use of the more constrained environments where distance-based control can be applied, making it more suitable for real world tasks. An introduction to multi-agent formation control is presented in Oh et al. (2015). In Wang et al. (2017) a decentralized formation control for underactuated vessels with a leader-follower

scheme is studied, desired relative positions to each agent are given. Peng et al. (2015) and Chu et al. (2017) consider the formation control problem for multiple non-holonomic mobile robots, achieving convergence to a desired moving formation, the positions of each agent in the formation are given. Time-varying formation tracking for high-order MAS with a directed topology is studied in Hua et al. (2018), formation and tracking of the desired trajectory in finite-time is achieved, desired relative positions of the followers are provided. In Mehdifar et al. (2018) following a leader-follower scheme, a single integrator MAS with a minimally and infinitesimally rigid graph, achieves formation maneuvering through a finite-time velocity estimator and rigidity-based distance-based formation maneuvering control, different from the above works only interagent distances are given, i.e. the relative positions between agents are not fixed, they adjust to fulfill the interagent restrictions, moreover the designed controllers are implementable in the local coordinate frames of the agents. Inspired by the aforementioned works, this paper considers a finite-time distance-based formation maneuvering problem for non-holonomic wheeled mobile robots with a minimally and infinitesimally rigid desired formation. It is assumed that at least two agents have access to the relative position of the leader, and at least one follower has access to the leader's velocity. To achieve the formation maneuvering objective,

inspired by Mehdifar et al. (2018), both a decentralized velocity estimator together with a rigidity-based formation controller are designed. The contributions of this paper are summarized as: (1) Finite-time rigidity-based formation acquisition applied to non-holonomic vehicles. (2) A reduced rigidity matrix  $\bar{R}$  is proposed to allow for leader-follower distance keeping. The designed estimator and controller guarantee convergence in finite-time and can be implemented in the local coordinate frames of the agents.

## 2. PRELIMINARIES

An undirected graph is defined as  $G \triangleq (V, E)$  where  $V = \{1, 2, \dots, n\}$  is the set of vertices and  $E \subset V \times V$  is the set of undirected edges in which if a vertex pair  $(i, j) \in E$  then so is  $(j, i) \in E$ . The number of elements in  $V$  and  $E$  is given by the cardinality of its sets denoted by  $|V| = n$ ,  $|E| = m$ . The adjacency matrix associated to the graph  $G$ , denoted by  $A(G)$  is the symmetric  $n \times n$  matrix whose elements are defined as:  $a_{ij} = 1$  if  $(i, j) \in E$ , otherwise  $a_{ij} = 0$ . Note that  $a_{ii} = 0$ . The neighborhood of a vertex  $i$  is the set  $\mathcal{N}_i = \{j \in V | (i, j) \in E\}$ . The degree matrix for the graph  $G$  is defined as  $D(G) = \text{diag}\{d_1, \dots, d_n\} \in \mathbb{R}^{n \times n}$  where  $d_i = \sum_{j=1}^n a_{ij}$ . The graph Laplacian associated with an undirected graph  $G$  is defined as Mesbahi and Egerstedt (2010):  $\mathcal{L}(G) = D(G) - A(G)$ . A framework is the pair  $\mathcal{F} \triangleq (G, \mathcal{P})$ , where  $G$  is a graph and  $\mathcal{P} = [\mathcal{P}_1^T, \dots, \mathcal{P}_n^T]^T$  is the set of positions that are assigned to each node, a map from  $V$  to  $\mathbb{R}^d$ , Mehdifar et al. (2018), Jackson (2007). A distance set  $\Delta = [\dots, \delta_{ij}, \dots]$ ,  $\delta_{ij} > 0 \in \mathbb{R}$ , is realizable if there exists a framework such that  $\|p_j - p_i\| = \delta_{ij} \quad \forall (i, j) \in E$ . A framework is said to be rigid if the corresponding realizable distance set constrains are sufficient to maintain the formation shape, Hendrickx et al. (2008), Izmetiev (2009). A minimally (min.) rigid framework is a rigid framework such that no edge of it's graph can be removed without losing rigidity, Hendrickx et al. (2008). An infinitesimally (inf.) rigid framework requires that given a velocity vector assigned to each vertex of the framework, the initial rate of change of the distance between each pair of vertices joined by an edge is zero, that is, preservation of inter-agent distances to the first-order during an infinitesimal motion, Izmetiev (2009).  $\mathbf{1}_n$  stands for the  $n \times 1$  vector of ones,  $I_n$  stands for the  $n \times n$  identity matrix and  $\otimes$  denotes the Kronecker product. The function  $\text{sig}(x)^\alpha$  of the real scalars  $x$ ,  $\alpha$  is defined as:  $\text{sig}(x)^\alpha = |x|^\alpha \text{sign}(x)$ . The functions  $\text{sign}(\mathbf{x})$  and  $\text{sig}(\mathbf{x})^\alpha$  of a vector  $\mathbf{x} \in \mathbb{R}^p$  are defined as:

$$\text{sign} \begin{bmatrix} x_1 \\ \vdots \\ x_p \end{bmatrix} = \begin{bmatrix} \text{sign}(x_1) \\ \vdots \\ \text{sign}(x_p) \end{bmatrix}, \quad \text{sig} \left( \begin{bmatrix} x_1 \\ \vdots \\ x_p \end{bmatrix} \right)^\alpha = \begin{bmatrix} \text{sig}(x_1)^\alpha \\ \vdots \\ \text{sig}(x_p)^\alpha \end{bmatrix}, \in \mathbb{R}^p \quad (1)$$

For a vector  $\mathbf{x} \in \mathbb{R}^n$ ,  $\|\mathbf{x}\|_2 = [\sum_{k=1}^n |x_k|^2]^{1/2}$  represents the 2-norm.  $\|\mathbf{x}\|_1 = \sum_{k=1}^n |x_k|$  denotes the 1-norm, and  $\|\mathbf{x}\|_p = [\sum_{k=1}^n |x_k|^p]^{1/p}$  denotes the p-norm.

*Lemma 1.* Mesbahi and Egerstedt (2010)[Geršgorin circle Theorem] Let  $\mathcal{A} \in \mathbb{C}^{n \times n}$  and let  $C_i$  be the closed circle in the complex plane centered at  $\mathcal{A}_{ii}$  with radius given by the row sum  $r_i = \sum_{j \neq i} |\mathcal{A}_{ij}|$ :  $C_i = \{z \in \mathbb{C} : |z - \mathcal{A}_{ii}| \leq r_i\}$ . Then all the eigenvalues of  $\mathcal{A}$  lie in the union of the circles  $C_i$  for  $i = 1, \dots, n$ .

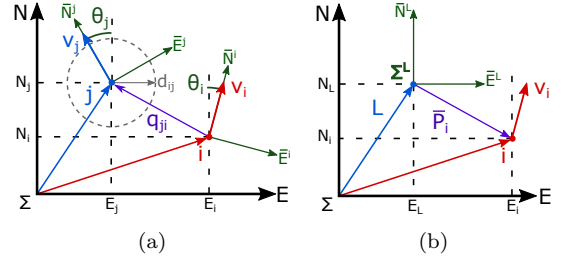


Fig. 1. 1a Position and orientation of two agents  $i$  and  $j$  in  $\Sigma$  and 1b Leader-fixed frame.

*Lemma 2.* If  $x_i \geq 0$ , then:  $(\sum_{i=1}^n x_i)^2 \geq \sum_{i=1}^n x_i^2$

*Lemma 3.* For a positive definite matrix  $\mathcal{B} \in \mathbb{R}^{n \times n}$ , and a vector  $\mathbf{x} \in \mathbb{R}^n$ :  $\lambda_{\min}(\mathcal{B})\|\mathbf{x}\|_2^2 \leq \mathbf{x}^T \mathcal{B} \mathbf{x} \leq \lambda_{\max}(\mathcal{B})\|\mathbf{x}\|_2^2$ . Where  $\lambda_{\min}$  and  $\lambda_{\max}$  are the minimum and maximum eigenvalues of the matrix  $\mathcal{B}$ .

*Lemma 4.* If  $x_i \leq 0$  and  $0 < \alpha < 1$ , then:

$$\sum_{i=1}^n (x_i^\alpha) > (\sum_{i=1}^n x_i)^\alpha$$

*Lemma 5.* [Hölder's inequality] For vectors  $x, y \in \mathbb{R}^n$ , positive real scalars  $p, q$  and the condition  $1/p + 1/q = 1$ , then:  $\|x^T y\|_1 \leq \|x\|_p \|y\|_q$ .

*Lemma 6.* [Young's inequality] For real scalars  $x, y$  and positive real scalars  $0 \leq \alpha, \beta \leq 1$  under the condition  $\alpha + \beta = 1$ , then:  $x^\alpha y^\beta \leq \alpha x + \beta y$ .

## 3. PROBLEM STATEMENT

Consider a MAS composed of  $n$  nonholonomic wheeled mobile robots, which can be modeled as:

$$\dot{\zeta}_i = [\dot{N}_i \quad \dot{E}_i \quad \dot{\theta}_i]^T = \begin{bmatrix} \cos \theta_i & 0 \\ \sin \theta_i & 0 \\ 0 & 1 \end{bmatrix} \begin{bmatrix} \nu_i \\ \omega_i \end{bmatrix} \quad (2)$$

where  $\zeta_i = [N_i \quad E_i \quad \theta_i]^T$  is the position and orientation of the  $i$ -th robot in an inertial Cartesian frame, and  $\nu_i, \omega_i, \theta_i$  are the linear velocity, the angular velocity and the heading angle respectively, all of them related to the Earth-Fixed North-East coordinate frame  $\Sigma$ , as shown in Fig. 1a. Also, denote  $P_i = [N_i \quad E_i]^T \in \mathbb{R}^2$ . Take the non-linear transformation  $\mathfrak{T}: \Gamma_i = \nu_i [C_{\theta_i} \quad S_{\theta_i}]^T$ , where  $\Gamma_i \triangleq [\Gamma_{i1} \quad \Gamma_{i2}]^T$ ,  $C_{\theta_i}$  and  $S_{\theta_i}$  denote  $\cos(\theta_i)$  and  $\sin(\theta_i)$  respectively, also  $-\pi \leq \theta \leq \pi$  and assuming the vehicles will be in continuous motion then  $\nu_i \neq 0$ . The transformation can be verified to be a diffeomorphism by taking its Jacobian:  $J(\mathfrak{T}) = \begin{bmatrix} C_{\theta_i} & -\nu_i S_{\theta_i} \\ S_{\theta_i} & \nu_i C_{\theta_i} \end{bmatrix}$ . With determinant  $\det(J(\mathfrak{T})) = \nu_i C_{\theta_i}^2 + \nu_i S_{\theta_i}^2 = \nu_i$ . Since we assumed  $\nu_i \neq 0$  then  $\det(J(\mathfrak{T})) \neq 0$  and  $J(\mathfrak{T})$  is nonsingular. So  $\Gamma_i$  is a local diffeomorphism in the defined set. Taking the time derivative of  $\Gamma_i$ :  $\dot{\Gamma}_i = \begin{bmatrix} C_{\theta_i} & -\nu_i S_{\theta_i} \\ S_{\theta_i} & \nu_i C_{\theta_i} \end{bmatrix} \begin{bmatrix} \dot{\nu}_i \\ \dot{\omega}_i \end{bmatrix} = \mathbb{A}_i U_i^*$ . Where  $\mathbb{A}_i \in \mathbb{R}^{2 \times 2}$  is an invertible matrix if  $\nu_i \neq 0$ . Then system (2) can be rewritten as:

$$\dot{P}_i = \Gamma_i, \quad \dot{\Gamma}_i = \mathbb{A}_i U_i^* \quad (3)$$

(3) can be viewed as a cascade connection, where  $\dot{P}_i$  has  $\Gamma_i$  as control input, and  $\Gamma_i$  has  $U_i^*$  as control input. Define the desired rigid formation with a min. and inf. rigid framework  $\mathcal{F}^* \triangleq (G^*, \mathcal{P}^*)$ , where  $G^* \triangleq (V^*, E^*)$  is the leader and followers graph, where movement of the leader vehicle is independent from the followers' motion and can send information to it's neighbors, the leader has bounded

velocity vector and angular velocity,  $v_L = [v_{LN} \ v_{LE}]^T$  and  $\omega_L$ , respectively, and bounded linear and angular accelerations,  $\dot{v}_L, \dot{\omega}_L$ , respectively, where the magnitude of  $\dot{v}_L$  is bounded by  $\|\dot{v}_L\|_2 \leq \gamma$ . Also for the Leader-Followers graph  $G^*$ ,  $|V^*| = n^*$ ,  $|E^*| = m^* = 2n^* - 3$ , since it is min. rigid. Considering only the followers, their graph is given by  $G \triangleq (V, E)$  which is assumed to be connected, and  $|V| = n = n^* - 1$ . For the formation control design it is assumed that each follower can measure their relative positions with their neighbors  $q_{ij} = p_j - p_i$ ,  $\forall j \in \mathcal{N}_i$ , and through on-board sensors and odometry estimate  $\zeta_i$  and  $\dot{\zeta}_i$ . The goal is to design finite-time distributed distance-based formation maneuvering controllers for the followers such that they, simultaneously, keep the desired distances to their neighbors and move cohesively with the leader. The control objectives are stated as:

$$e_{ij} = \|P_i - P_j\| - \delta_{ij} = 0, \quad v_i = v_L \quad (4)$$

where  $(i, j) \in E^*$ . These represent the objectives: to keep a desired distance  $\delta_{ij}$  between neighbor agents and for all agents to move at the leader's velocity. Since the graph is required to be inf. rigid, if the desired inter-agent distances are kept then the agents will maintain formation and move cohesively. The vector  $e$  is ordered such that  $i < j$ ,  $(i, j) \in V$ . Then:  $e = [\dots, e_{Lk}, \dots, e_{ij}, \dots]^T \in \mathbb{R}^{m^*}$  where  $k \in \mathcal{N}_L$  and  $(i, j) \in V$ . This ordering will prove to be useful in the arrangement of  $\eta$ ,  $R$  and  $\bar{R}$ . Define:

$$\eta_{ij} = \|P_i - P_j\|^2 - \delta_{ij}^2 = e_{ij}(e_{ij} + 2\delta_{ij}) \quad (5)$$

Note that  $\eta_{ij}$  is zero if and only if  $e_{ij} = 0$ , i.e. when the control objective is reached. Therefore control objectives (4), are achieved by driving  $\eta$  to zero.

## 4. FINITE-TIME FORMATION MANEUVERING

### 4.1 Finite-Time leader velocity estimator

For each agent, the following estimator is proposed to estimate the leader's velocity vector  $v_L = [v_{LN} \ v_{LE}]^T$ :

$$\begin{aligned} \dot{\hat{v}}_i = & -k_1 \left( \sum_{j \in \mathcal{N}_i} [a_{ij} (\hat{v}_i - \hat{v}_j)] + b_i (\hat{v}_i - v_L) \right) \\ & - k_2 \text{sign} \left( \sum_{j \in \mathcal{N}_i} [a_{ij} (\hat{v}_i - \hat{v}_j)] + b_i (\hat{v}_i - v_L) \right) \end{aligned} \quad (6)$$

where  $\hat{v}_i = [\hat{v}_{iN} \ \hat{v}_{iE}]^T$  with  $\hat{v}_{iN}$  and  $\hat{v}_{iE}$  being the north and east components of the  $i$ th agent's estimate of  $v_L$ , and  $j \in \mathcal{N}_i$ . Note that  $a_{ij}$  are elements of the matrix  $A(G)$ ,  $b_i$  represents connectivity between agent  $i$  and the leader, if information is received by the follower then  $b_i = 1$ , otherwise  $b_i = 0$ , it is assumed that at least one agent has a connection with the leader, and  $k_1, k_2$  are positive scalars. The following matrices related to the graph  $G$  are defined:  $D_2 = D \otimes I_2$ ,  $A_2 = A \otimes I_2$ ,  $\mathcal{L}_2 = \mathcal{L} \otimes I_2$ ,  $B = \text{diag}(b_1, \dots, b_n)$  and  $B_2 = B \otimes I_2$ . It is evident that:  $\mathcal{L}_2 = D_2 - A_2$ . Taking  $\mathcal{H} = \mathcal{L} + B$  and  $\mathcal{H}_2 = \mathcal{H} \otimes I_2$ , it follows that  $\mathcal{H}_2 = \mathcal{L}_2 + B_2$ . Also define  $\tilde{V} = [\hat{v}_1^T \dots \hat{v}_n^T]^T$  as the column vector of the followers' estimates and  $V_L = \mathbf{1}_n \otimes v_L = [v_L^T, \dots, v_L^T]^T \in \mathbb{R}^{2n}$ . All the equations are understood in the Filippov sense in order to provide for the possibility to use discontinuous sign function. Shtessel et al. (2014).

*Theorem 1.* Let  $\mathcal{H}_2$  be a real symmetric matrix. Under the assumptions that the followers' graph is connected and at least one follower has access to  $V_L$ . The estimator (6) drives  $\tilde{V}$  to  $V_L$  in finite-time  $T_0 = 2\mathcal{V}_{C1}(\tilde{V}(0))^{1/2}/K_{C1}$  where:  $K_{C1} = (-\sqrt{2}(k_2 - \gamma)\lambda_{\min}(\mathcal{H}_2))/\sqrt{\lambda_{\max}(\mathcal{H}_2)}$ , by selecting:  $k_2 > \gamma$ .  $\mathcal{V}_{C1} = \frac{1}{2}\tilde{V}^T \mathcal{H}_2 \tilde{V}$  is a positive definite and radially unbounded Lyapunov candidate function.

**Proof.** Adding and subtracting  $v_L$  in (6) and considering  $\sum_{j \in \mathcal{N}_i} [a_{ij}] = d_i$ , then (6) is rewritten for the whole system in matrix form as:  $\dot{\tilde{V}} = -k_1[\mathcal{H}_2(\tilde{V} - V_L)] - k_2 \text{sign}[\mathcal{H}_2(\tilde{V} - V_L)]$ . Let  $\tilde{V} = \hat{V} - V_L \rightarrow \dot{\tilde{V}} = \dot{\hat{V}} - \dot{V}_L$  then:

$$\dot{\tilde{V}} = -k_1(\mathcal{H}_2 \tilde{V}) - k_2 \text{sign}(\mathcal{H}_2 \tilde{V}) - \dot{V}_L \quad (7)$$

By Lemma 1, for a connected graph,  $\mathcal{H}$  is positive definite, Hu and Hong (2007).  $\mathcal{H}_2$  is also positive definite as by Kronecker product properties the eigenvalues remain the same. Taking the time derivative of  $\mathcal{V}_{C1}$ :  $\dot{\mathcal{V}}_{C1} = \tilde{V}^T \mathcal{H}_2 \dot{\tilde{V}}$

$$\dot{\mathcal{V}}_{C1} = -k_1 \tilde{V}^T \mathcal{H}_2^2 \tilde{V} - k_2 \tilde{V}^T \mathcal{H}_2 \text{sign}(\mathcal{H}_2 \tilde{V}) - \tilde{V}^T \mathcal{H}_2 \dot{V}_L \quad (8)$$

Where  $\mathcal{H}_2^2 = \mathcal{H}_2 \mathcal{H}_2$ . Note that  $[\mathcal{H}_2 \tilde{V}]$  is a  $2n \times 1$  vector, the subscript  $\ell$  will be used to indicate an element of this vector. When  $\ell$  is odd, the element corresponds to the north component, and to the east component when it is even. Therefore (8) can be rewritten as:  $\dot{\mathcal{V}}_{C1} = -k_1 \tilde{V}^T \mathcal{H}_2^2 \tilde{V} - k_2 \sum_{\ell=1}^{2n} |[\mathcal{H}_2 \tilde{V}]_\ell| - \dot{v}_{LN} \sum_{i=1}^n |[\mathcal{H}_2 \tilde{V}]_{2i-1}| - \dot{v}_{LE} \sum_{i=1}^n |[\mathcal{H}_2 \tilde{V}]_{2i}|$ . Since the magnitude of  $\dot{V}_L$  is bounded:

$$\dot{\mathcal{V}}_{C1} < -k_1 \tilde{V}^T \mathcal{H}_2^2 \tilde{V} - (k_2 - \gamma) \sum_{\ell=1}^{2n} |[\mathcal{H}_2 \tilde{V}]_\ell| \quad (9)$$

If  $k_2 > \gamma$  then  $\dot{\mathcal{V}}_{C1}$  is negative definite  $\forall \tilde{v} \neq 0$ , also since  $\mathcal{V}_{C1}$  is radially unbounded, the origin of  $\tilde{V}$  is globally asymptotically stable. Therefore  $\tilde{V} \rightarrow 0$  as  $t \rightarrow \infty$ . From (9), the definition of the 2-norm and Lemma 2, the following can be obtained:

$$\dot{\mathcal{V}}_{C1} \leq -(k_2 - \gamma) \left\| [\mathcal{H}_2 \tilde{V}] \right\|_1 \leq -(k_2 - \gamma) \left\| [\mathcal{H}_2 \tilde{V}] \right\|_2 \quad (10)$$

From (10) and Lemma 3, the origin of  $\tilde{V}$  is globally exponentially stable, moreover (7) is input-to-state stable (ISS), Khalil (2014). Consider Lemma 3 on (10), thus:

$$\dot{\mathcal{V}}_{C1} \leq \frac{-(k_2 - \gamma)\lambda_{\min}(\mathcal{H}_2)(\lambda_{\max}(\mathcal{H}_2)\|\tilde{V}\|_2^2)^{1/2}}{(\lambda_{\max}(\mathcal{H}_2))^{1/2}} \quad (11)$$

Considering that:  $(2\mathcal{V}_{C1})^{1/2} \leq \sqrt{\lambda_{\max}(\mathcal{H}_2)} \|\tilde{V}\|_2^2$ .

Then, (11) becomes:  $\dot{\mathcal{V}}_{C1} \leq \frac{-(k_2 - \gamma)\lambda_{\min}(\mathcal{H}_2)}{\sqrt{\lambda_{\max}(\mathcal{H}_2)}} \sqrt{2\mathcal{V}_{C1}}$ . From which the following can be obtained:  $2\mathcal{V}_{C1}(\tilde{V}(t))^{1/2} \leq 2\mathcal{V}_{C1}(\tilde{V}(0))^{1/2} - \frac{-\sqrt{2}(k_2 - \gamma)\lambda_{\min}(\mathcal{H}_2)}{\sqrt{\lambda_{\max}(\mathcal{H}_2)}} t$ . When  $\tilde{V} = 0$  then

$\mathcal{V}_{C1}(\tilde{V}) = 0$ , thus  $t \leq T_0 = \frac{2\mathcal{V}_{C1}(\tilde{V}(0))^{1/2}}{K_{C1}}$  where:  $K_{C1} = \frac{-\sqrt{2}(k_2 - \gamma)\lambda_{\min}(\mathcal{H}_2)}{\sqrt{\lambda_{\max}(\mathcal{H}_2)}}$ . This implies that (6) drives  $\hat{V} \rightarrow V_L$  in finite-time  $T_0$ . ■

### 4.2 Finite-Time Controller Design

From (4), the error dynamics is given by:  $\dot{e}_{ij} = [P_i - P_j]^T (\dot{P}_i - \dot{P}_j)/(e_{ij} + \delta_{ij})$ . And from (5) the dynamic of  $\eta_{ij}$

is:  $\dot{\eta}_{ij} = 2[P_i - P_j]^T(\dot{P}_i - \dot{P}_j)$ ;  $(i, j) \in E^*$ . The rigidity matrix  $R(P)$  of the Framework  $\mathcal{F}^*$  is a real matrix with  $m^*$  rows and  $2n^*$  columns, both with the appropriate ordering. Thus each row is associated with an edge, and each pair of columns with a vertex. The row corresponding to edge  $(i, j) \in E^*$  where  $i < j$ , has the form, Jackson (2007):  $[0_2^T, \dots, (P_i - P_j)^T, \dots, 0_2^T, \dots, (P_j - P_i)^T, \dots, 0_2^T]$ . The vector  $\eta$  has the same ordering as  $e$ , with dynamics:

$$\dot{\eta} = 2R[\dot{P}_L \ \dot{P}]^T \quad (12)$$

Where  $\dot{P} = [\dot{P}_1^T \dots \dot{P}_n^T]^T \in \mathbb{R}^{2n}$ , and  $\dot{P}_L = [\dot{N}_L \ \dot{E}_L]^T \in \mathbb{R}^2$ . Notice that the row order of  $R$  is associated with the ordering of  $\eta$ , and the column order with  $[\dot{P}_L^T \ \dot{P}^T]^T$ . By substituting (3) into (12) we have the new system

$$\dot{\eta} = 2R[\dot{P}_L \ \Gamma]^T, \quad \dot{\Gamma} = \mathbb{A}U^* \quad (13)$$

Where  $\Gamma = [\Gamma_1^T, \dots, \Gamma_n^T]^T \in \mathbb{R}^{2n}$ ,  $\mathbb{A}$  is a nonsingular block diagonal matrix  $\mathbb{A} = \text{diag}\{\mathbb{A}_1, \dots, \mathbb{A}_n\} \in \mathbb{R}^{2n \times 2n}$ , and  $U^* = [U_1^{*T}, \dots, U_n^{*T}] \in \mathbb{R}^{2n}$ . This system can be viewed as a cascade connection, through backstepping a virtual control  $\Gamma = \xi$  that drives  $\eta$  to 0 is designed.

*Theorem 2.* The system (13) is driven to its origin in a finite settling-time  $T_f = T_0 + T_1$ , where  $T_1$  is upper bounded by  $T_1 \leq \frac{(1-\alpha)\mathcal{V}_{C2}(\eta(T_0))^{\frac{1-\alpha}{1+\alpha}}}{\mathcal{K}_3(1-\alpha)}$  with the control law:

$$U^* = -\mathbb{A}^{-1} \left( \bar{R}[\text{sig}(\eta)^\alpha] - \dot{\xi} + k_4 \text{sig}(\Lambda)^{\left(\frac{3\alpha-1}{\alpha+1}\right)} \right) \quad (14)$$

where  $\dot{\xi}$  is the time derivative of

$$\xi = -k_3 \bar{R}^T \text{sig}(\eta)^\alpha + \hat{V} \quad (15)$$

By selecting  $k_3, k_4$  as positive real scalars and being  $\bar{R}$  the reduced rigidity matrix as shown in (18),  $\Lambda = \Gamma - \xi$  and  $\frac{1}{3} < \alpha < 1$ .  $\mathcal{V}_{C2} = \sum_{(i,j) \in E^*} \left[ \frac{1}{(2(\alpha+1))} |\eta_{ij}|^{\alpha+1} \right]$  is a Lyapunov candidate function.  $\mathcal{K}_3$  is as shown in (22).

**Proof.** Note that (15) uses the velocity estimate  $\hat{V}$ . Expressing the position of each agent relative to a leader-fixed frame  $\Sigma^L$  with the same orientation as the earth-fixed frame, as shown in Fig. 1b, the relative position and velocity of the leader is:  $\bar{P}_L = [0 \ 0]^T \rightarrow \dot{\bar{P}}_L = [0 \ 0]^T$ . For the followers:  $\bar{P}_i = P_i - P_L \rightarrow \dot{\bar{P}}_L = \dot{P}_i - \dot{P}_L$ . Defining  $\bar{e}_{ij} = \|\bar{P}_i - \bar{P}_j\| - \delta_{ij} = \|\bar{q}_{ij}\| - \delta_{ij}$ . Where  $\bar{q}_{ij} = \bar{P}_i - \bar{P}_j$ , and  $(i, j) \in E^*$ . Then the error dynamic is  $\dot{\bar{e}}_{ij} = (\bar{q}_{ij}^T \dot{\bar{q}}_{ij}) / (\bar{e}_{ij} + \delta_{ij})$ . Now define

$$\bar{\eta}_{ij} = \|\bar{P}_i - \bar{P}_j\|^2 - \delta_{ij}^2 = \bar{e}_{ij}(\bar{e}_{ij} + 2\delta_{ij}) \quad (16)$$

With dynamics  $\dot{\bar{\eta}}_{ij} = 2\bar{q}_{ij}^T \dot{\bar{q}}_{ij} = 2(\bar{P}_i - \bar{P}_j)^T(\dot{P}_i - \dot{P}_j)$ . Note that  $\bar{e}_{Lk} = \|\bar{P}_L - \bar{P}_k\| - \delta_{kL} = \|P_L - P_k\| - \delta_{Lk} = e_{Lk}$ , where  $k \in \mathcal{N}_L$ . And  $\bar{e}_{ij} = \|\bar{P}_i - \bar{P}_j\| - \delta_{ij} = \|P_i - P_j\| - \delta_{ij} = e_{ij}$ , where  $(i, j) \in E$ . Then the relative distance error, its dynamic, and the relative position are the same in both frames  $\Sigma^L$  and  $\Sigma$ , written as:

$$\bar{e} = e, \quad \dot{\bar{e}} = \dot{e}, \quad \bar{q} = q \quad (17)$$

$\bar{\eta}$  has the same ordering as  $\eta$ , so  $\dot{\bar{\eta}} = [\dots, \dot{\bar{\eta}}_{Lk}, \dots, \dot{\bar{\eta}}_{ij}, \dots]^T$  where  $\dot{\bar{\eta}}_{Lk}$  correspond to edges connecting the leader with some (maybe all) followers, but at least 2, and  $\dot{\bar{\eta}}_{ij}$  correspond to edges between followers. Therefore  $\dot{\bar{\eta}}$  can be rewritten in matrix form as:

$$\dot{\bar{\eta}} = 2 \begin{bmatrix} \vdots \\ 0_2^T \dots \dots \dots \bar{P}_k^T \dots \dots \dots 0_2^T \\ \vdots \\ 0_2^T \dots [\bar{P}_i - \bar{P}_j]^T \dots 0_2^T \dots [\bar{P}_j - \bar{P}_i]^T \dots 0_2^T \\ \vdots \\ \vdots \end{bmatrix} \begin{bmatrix} \dot{\bar{P}}_1 \\ \vdots \\ \dot{\bar{P}}_n \end{bmatrix} \quad (18)$$

$$\dot{\bar{\eta}} = 2\bar{R}\dot{\bar{P}} \quad (19)$$

Denoting the matrix as  $\bar{R} \in \mathbb{R}^{m^* \times 2n}$  and  $\dot{\bar{P}} = [\dot{\bar{P}}_1^T \dots \dot{\bar{P}}_n^T]^T \in \mathbb{R}^{2n}$ . The rows of  $\bar{R}$  have the same order as  $\bar{\eta}$ . Infinitesimal rigidity is checked, for followers connected to the leader, the inf. rigidity condition is:  $\bar{V}_k \cdot \bar{P}_k = 0$ . The set of  $\bar{V}_k$  that satisfies the equation is  $\bar{V}_k = 0$  or  $\bar{V}_k \perp \bar{P}_k$ . For the followers:  $(\bar{P}_i - \bar{P}_j) \cdot (\bar{V}_i - \bar{V}_j) = 0$ . Writing these in matrix form:  $\bar{R}\bar{V} = 0$ . Where  $\bar{V} = [\bar{V}_1 \dots \bar{V}_n]^T$ . The set of  $\bar{V}$  that fulfills this condition is  $\text{Null}(\bar{R})$ , and the degrees of freedom (DOF) in  $\bar{V}$ , is  $\text{nullity}(\bar{R})$ . For a fixed position leader, the DOF of the framework is 1, a rotation around the leader, then  $\text{nullity}(\bar{R}) = 1$ . By the rank-nullity theorem:  $\text{Rank}(\bar{R}) = (2n^* - 2) - 1 = 2n^* - 3 = m^*$ . Therefore  $\bar{R}$  is full row rank and full rank. Considering  $\bar{q} = q$ ,  $\dot{\bar{\eta}}$  can be rewritten as:

$$\dot{\bar{\eta}} = 2\bar{R}\bar{U} \quad (19)$$

Where  $\bar{U} = [(\dot{P}_1 - \dot{P}_L)^T \dots (\dot{P}_n - \dot{P}_L)^T]^T$ . Consider the potential function, Mehdifar et al. (2018)  $\mathcal{V}_{ij} = [1/(2(\alpha+1))] |\bar{\eta}_{ij}|^{\alpha+1}$ . For  $\frac{1}{3} < \alpha < 1$ ,  $(i, j) \in E^*$ .  $\mathcal{V}_{ij}$  is positive definite and since  $\bar{e}_{ij}$  is defined on  $[-\delta_{ij}, \infty]$  and  $\bar{\eta}$  is a function of  $\bar{e}_{ij}$  then  $\mathcal{V}_{ij}$  is also radially unbounded. Define  $\mathcal{V}_{C2} = \sum_{(i,j) \in E^*} \mathcal{V}_{ij}$  and take its time derivative along the system trajectories:

$$\dot{\mathcal{V}}_{C2} = [\text{sig}(\bar{\eta})^\alpha]^T \bar{R}\bar{U} \quad (20)$$

Choosing the virtual control  $\bar{U} = -k_3 \bar{R}^T \text{sig}(\bar{\eta})^\alpha$ , where  $\frac{1}{3} < \alpha < 1$  and  $k_3 > 0$ . Then (20) with control  $\bar{U}$  is:  $\dot{\mathcal{V}}_{C2} = -k_3 [\text{sig}(\bar{\eta})^\alpha]^T \bar{R}\bar{R}^T \text{sig}(\bar{\eta})^\alpha$ . Since the framework is inf. rigid, and  $\bar{R}$  is full rank, then  $\bar{R}\bar{R}^T \geq 0$ ; also  $\text{Rank}(\bar{R}\bar{R}^T) = \text{Rank}(\bar{R})$ , hence  $\bar{R}\bar{R}^T$  is full rank, which means it is nonsingular, so we conclude  $\bar{R}\bar{R}^T > 0$ . Then  $\dot{\mathcal{V}}_{C2} = -k_3 [\text{sig}(\bar{\eta})^\alpha]^T \bar{R}\bar{R}^T \text{sig}(\bar{\eta})^\alpha < 0$ . And since  $\mathcal{V}_{C2}$  is radially unbounded, then the origin is globally asymptotically stable. From Lemma 3,  $\dot{\mathcal{V}}_{C2}$  can be written as:

$$\dot{\mathcal{V}}_{C2} \leq -k_3 \lambda_{\min}(\bar{R}\bar{R}^T) [\text{sig}(\bar{\eta})^\alpha]^T [\text{sig}(\bar{\eta})^\alpha] \quad (21)$$

Note that  $0 < (2\alpha/[1+\alpha]) < 1$ . Using Lemma 4:  $[\text{sig}(\bar{\eta})^\alpha]^T [\text{sig}(\bar{\eta})^\alpha] \geq (\sum_{(i,j) \in E^*} |\bar{\eta}_{ij}|^{1+\alpha})^{2\alpha/1+\alpha}$ . Also from  $\mathcal{V}_{C2}$  and the previous result:  $[\text{sig}(\bar{\eta})^\alpha]^T [\text{sig}(\bar{\eta})^\alpha] \leq [2(\alpha+1)] \left( \frac{2\alpha}{1+\alpha} \right) \mathcal{V}_{C2}^{\left(\frac{2\alpha}{1+\alpha}\right)}$ . Then (21) can be rewritten as:

$$\dot{\mathcal{V}}_{C2} \leq -k_3 [2(\alpha+1)]^{\left(\frac{2\alpha}{1+\alpha}\right)} \lambda_{\min}(\bar{R}\bar{R}^T) \mathcal{V}_{C2}^{\left(\frac{2\alpha}{1+\alpha}\right)} = -\mathcal{K}_3 \mathcal{V}_{C2}^{\left(\frac{2\alpha}{1+\alpha}\right)} \quad (22)$$

Where  $\mathcal{K}_3 = k_3 [2(\alpha+1)]^{\left(\frac{2\alpha}{1+\alpha}\right)} \lambda_{\min}(\bar{R}\bar{R}^T) > 0$ . From Lemma 5 in Mehdifar et al. (2018) and (22) we conclude that  $\bar{\eta} \rightarrow 0$  in finite-time  $T_1$ , where  $T_1 \leq \frac{(1-\alpha)\mathcal{V}_{C2}(\bar{\eta}(T_0))^{\frac{1-\alpha}{1+\alpha}}}{\mathcal{K}_3(1-\alpha)}$ . Considering (16) we conclude  $\bar{\eta} = \eta$ , as  $\bar{\eta} \rightarrow 0$ , thus  $\eta \rightarrow 0$  in finite-time and  $\eta$  has a globally asymptotically stable origin. Considering  $\bar{U}$  as a virtual input and since by  $t > T_0$ ,  $\hat{V} = V_L$ , then  $\bar{U} = \xi - \dot{P}_L \Rightarrow \xi = \bar{U} + V_L = \bar{U} + \hat{V}$ . Which for each follower:

$$\xi_i = -k_3 \sum_{j \in \mathcal{N}_i} [(P_i - P_j) \text{sig}(\eta_{ij})^\alpha] + \hat{v} \quad (23)$$

Now that a control  $\xi = [\xi_1^T, \dots, \xi_n^T]^T \in \mathbb{R}^{2n}$  stabilizes  $\eta$ , and  $\dot{\mathcal{V}}_{C2} \leq -W_2$ , is known, where  $W_2$  is a positive definite function, the control  $U^*$  that drives  $\Gamma$  to  $\xi$  is designed.  $\forall t \geq T_0$ ,  $\hat{V} = V_L$ , rewriting  $\dot{\eta}$  using (15), and the fact that  $R\mathbf{a} = 0$  if  $\mathbf{a} = [a, \dots, a]^T \in \mathbb{R}^{2n^*}$ , we obtain:  $\dot{\eta} = 2R[0_2^T \bar{U}^T]^T$ . Note that for a vector  $x \in \mathbb{R}^{2n}$  and the rigidity matrix  $R$ , the following result holds:  $R[0_2^T x^T]^T = \bar{R}x$ . Therefore we can rewrite  $\dot{\eta}$  as  $\dot{\eta} = 2\bar{R}\bar{U}$ . Similar to (19). Taking (13), adding and subtracting  $\xi$  from  $\Gamma$ :  $\dot{\eta} = 2\bar{R}\bar{U} + 2\bar{R}(\Gamma - \xi)$ . Taking the change of variables  $\Lambda = \Gamma - \xi$  results in the system:

$$\dot{\eta} = 2\bar{R}\bar{U} + 2\bar{R}\Lambda, \quad \dot{\Lambda} = \Lambda U^* - \dot{\xi} \quad (24)$$

Choosing the radially unbounded Lyapunov candidate function:  $\mathcal{V}_{C3} = \mathcal{V}_{C2} + \frac{1}{2}\Lambda^T\Lambda$ , and taking its time derivative:  $\dot{\mathcal{V}}_{C3} \leq -W_2 + \Lambda^T(\bar{R}^T[\text{sig}(\eta)^\alpha] + \Lambda U^* - \dot{\xi})$ . Choosing  $U^* = -\Lambda^{-1}(\bar{R}[\text{sig}(\eta)^\alpha] - \dot{\xi} + k_4 \text{sig}(\Lambda)^{\frac{3\alpha-1}{\alpha+1}})$  with  $\frac{1}{3} < \alpha < 1$  then:  $\dot{\mathcal{V}}_{C3} \leq -W_2 - k_4 \Lambda^T \text{sig}(\Lambda)^{\frac{3\alpha-1}{\alpha+1}}$ . Denoting the  $\ell$ -th scalar element of  $\Lambda$  as  $\Lambda_\ell$  to prevent confusion with the  $2 \times 1$  vector  $\Lambda_i$ , then:  $\dot{\mathcal{V}}_{C3} \leq -W_2 - k_4 \sum_{\ell=1}^{2n} (|\Lambda_\ell|^2)^{\frac{2\alpha}{\alpha+1}}$ . From Lemma 4 we have:  $\sum_{\ell=1}^{2n} (|\Lambda_\ell|^2)^{\frac{2\alpha}{\alpha+1}} > [\sum_{\ell=1}^{2n} (|\Lambda_\ell|^2)]^{\frac{2\alpha}{\alpha+1}}$ . Taking  $W_2 = \mathcal{K}_3 \mathcal{V}_{C2}^{(2\alpha/\alpha+1)}$  and  $\mathcal{V}_C = \frac{1}{2}\Lambda^T\Lambda = \frac{1}{2} \sum_{\ell=1}^{2n} (\Lambda_\ell^2)$ ,  $\dot{\mathcal{V}}_{C3}$  can be rewritten as:  $\dot{\mathcal{V}}_{C3} \leq -\mathcal{K}_3 \mathcal{V}_{C2}^{\frac{2\alpha}{\alpha+1}} - \mathcal{K}_4 \mathcal{V}_C^{\frac{2\alpha}{\alpha+1}}$  Where  $\mathcal{K}_4 = 2^{\frac{2\alpha}{\alpha+1}} k_4$ . Defining the positive real scalar  $\mathcal{K}_5 \leq \min(\mathcal{K}_3, \mathcal{K}_4)$ , then  $\dot{\mathcal{V}}_{C3} \leq -\mathcal{K}_5 (\mathcal{V}_{C2}^{\frac{2\alpha}{\alpha+1}} + \mathcal{V}_C^{\frac{2\alpha}{\alpha+1}})$  Since  $\mathcal{V}_{C3} = \mathcal{V}_{C2} + \mathcal{V}_C$  then  $\mathcal{C}\mathcal{V}_{C3}^\beta = \mathcal{C}(\mathcal{V}_{C2} + \mathcal{V}_C)^\beta$  where  $\mathcal{C}$  is a real positive scalar and  $0 < \beta < 1$ . From Lemma 4:  $(\mathcal{V}_{C2} + \mathcal{V}_C)^\beta < (\mathcal{V}_{C2}^\beta + \mathcal{V}_C^\beta)$  thus  $\mathcal{C}\mathcal{V}_{C3}^\beta < \mathcal{C}(\mathcal{V}_{C2}^\beta + \mathcal{V}_C^\beta)$ , then:  $\dot{\mathcal{V}}_{C3} \leq -\mathcal{K}_5 \mathcal{V}_{C3}^{\frac{2\alpha}{\alpha+1}}$ .  $\dot{\mathcal{V}}_{C3}$  is negative definite, therefore  $\eta \rightarrow 0$  and  $\Lambda \rightarrow 0$ , so the origin of (24) is globally asymptotically stable, moreover from Lemma 5 in Mehdifar et al. (2018) the origin is reached in finite-time  $T_2$ .  $\Lambda \rightarrow 0$  implies  $\Gamma \rightarrow \xi$ .  $\dot{\xi}$  is computed by means of the First-Order Sliding Mode differentiator proposed in Levant (2003). Consider the time interval  $0 \leq t \leq T_0$ . Rewriting  $\dot{\eta}$  using the input (15) yields  $\dot{\eta} = 2\bar{R}(\bar{U} + \tilde{V})$ . Which can be written as:

$$\dot{\eta} = 2\bar{R}\bar{U} + 2\bar{R}\Lambda + 2\bar{R}\tilde{V}, \quad \dot{\Lambda} = \Lambda U^* - \dot{\xi} \quad (25)$$

This creates a cascade system, given the Lyapunov candidate function  $\mathcal{V}_{C3}$ , taking its time derivative:

$$\dot{\mathcal{V}}_{C3} = \frac{1}{2} [\text{sig}(\eta)^\alpha]^T (2\bar{R}\bar{U} + 2\bar{R}\Lambda + 2\bar{R}\tilde{V}) + \Lambda^T (\Lambda U^* - \dot{\xi}) \quad (26)$$

Define the vector  $Z^T = [\text{sig}(\eta)^\alpha]^T \bar{R} \in \mathbb{R}^{2n}$ , then  $k_3 [\text{sig}(\eta)^\alpha]^T \bar{R}\tilde{V} = k_3 Z^T \tilde{V}$ , applying Lemma 5 with  $p = q = 2$ , and Lemma 6 results in:  $k_3 [\text{sig}(\eta)^\alpha]^T \bar{R}\tilde{V} \leq \frac{k_3^2}{2} ([\text{sig}(\eta)^\alpha]^T \bar{R}\bar{R}^T \text{sig}(\eta)^\alpha) + \frac{1}{2} (\tilde{V}^T \tilde{V})$ . Multiply (26) by  $k_3$  on both sides and substitute the above results, dividing by  $k_3$ , using Lemma 3, writing in norm notation and noting that  $[\text{sig}(\eta)^\alpha]^T [\text{sig}(\eta)^\alpha] = \|\eta\|_{2\alpha}^{2\alpha}$ , yields  $\dot{\mathcal{V}}_{C3} \leq -\frac{k_3}{2} \lambda_{\min} [\bar{R}\bar{R}^T] \|\eta\|_{2\alpha}^{2\alpha} - k_4 \|\Lambda\|_{\frac{4\alpha}{\alpha+1}} + \frac{1}{2k_3} \|\tilde{V}\|_2^2$ . From Corollary 5.10 in Ding (2013), (25) is ISS with respect to the input  $\tilde{V}$ . Since (25) and (7) are ISS, then the cascade connection between (25) and (7) is ISS, Khalil (2014). So, the system (13) is stable while  $\hat{V} \rightarrow V_L$  on  $t \leq T_0$ , then for

$t > T_0$ ,  $\hat{V}$  follows  $V_L$  and  $\eta \rightarrow 0$  in finite-time, achieving the control objective. ■

### 4.3 Results in local frames

These results are given in Earth-Fixed coordinates, in a similar fashion to Mehdifar et al. (2018) we show that they can be expressed in local frames and that both the velocity estimator and the formation control are distributed.

*Velocity Estimator.*  $\hat{v}_i$  can be computed from integration of (6), as each agent can estimate its inertial orientation, the velocity estimations can be communicated in inertial coordinates which can then be expressed in the local frame of the agent  $i$  through the rotation matrix from the inertial frame to the local frame  $\mathcal{R}_i$ . Let the superscript  $i$  indicate a quantity expressed in the local frame of the  $i$ -th agent, then the local velocity estimate of the agent  $i$  is:  $\hat{v}_i^i = \mathcal{R}_i \hat{v}_i$

*Formation Control.* With a local velocity estimate  $\hat{v}_i^i$ , virtual control law (23) can be expressed in local coordinates:  $\xi_i^i = \mathcal{R}_i \xi_i = -k_3 \sum_{j \in \mathcal{N}_i} \mathcal{R}_i [q_{ij} \text{sig}(\eta_{ij})^\alpha] + \hat{v}_i^i = -k_3 \sum_{j \in \mathcal{N}_i} [q_{ij}^i \text{sig}(\eta_{ij}^i)^\alpha] + \hat{v}_i^i$ . Since  $\eta_{ij}$  depends only on relative distances, it is independent of the frame, thus  $\eta_{ij} = \eta_{ij}^i$ .  $q_{ij}^i$  is the locally measured relative position, then the virtual control law can be implemented locally. (14) can be written for each agent as:  $U_i^* = -\Lambda_i^{-1} \left( \sum_{j \in \mathcal{N}_i} [q_{ij} \text{sig}(\eta_{ij})^\alpha] - \dot{\xi}_i + k_4 \text{sig}(\Lambda_i)^{\frac{3\alpha-1}{\alpha+1}} \right)$ . In local coordinates it takes the form:  $U_i^{i*} = -\mathcal{R}_i \Lambda_i^{-1} \left( \sum_{j \in \mathcal{N}_i} [q_{ij}^i \text{sig}(\eta_{ij}^i)^\alpha] - \dot{\xi}_i^i + k_4 \text{sig}(\Lambda_i^i)^{\frac{3\alpha-1}{\alpha+1}} \right)$ . Where  $\Lambda_i^i = \mathcal{R}_i \Lambda_i - \xi_i^i = [0] - \xi_i^i$ . As  $\theta_i$  can be estimated on-board,  $\Lambda_i^{-1}$  can be computed,  $\xi_i^i$  can be calculated in the same way as  $\dot{\xi}_i$ . Hence the control law can be implemented locally.

## 5. SIMULATION RESULTS

Consider a MAS system with 4 agents and one leader, the communication and formation graph is shown in Fig. 2. Each robot can obtain information only from its neighbors, and agents 1 and 2 have access to  $v_L$ . The desired distances between agents are  $d_{ij} = 1$ . The agents' initial velocities are set to zero. Initial positions are:  $P_L = (0, 0)$ ,  $P_1 = (3, -3)$ ,  $P_2 = (-4, -3)$ ,  $P_3 = (3, -6)$ ,  $P_4 = (-4, -7)$ . From the graph, the sets  $V$ ,  $E$  and  $E^*$  are given by:

$$V = \{1, 2, 3, 4\} \quad E = \{(1, 2), (1, 3), (2, 3), (2, 4), (3, 4)\} \\ E^* = \{(L, 1), (L, 2), (1, 2), (1, 3), (2, 3), (2, 4), (3, 4)\}$$

Also the following matrices can be obtained:

$$A(G) = \begin{bmatrix} 0 & 1 & 1 & 0 \\ 1 & 0 & 1 & 1 \\ 1 & 1 & 0 & 1 \\ 0 & 1 & 1 & 0 \end{bmatrix}, \quad D(G) = \begin{bmatrix} 2 & 0 & 0 & 0 \\ 0 & 3 & 0 & 0 \\ 0 & 0 & 3 & 0 \\ 0 & 0 & 0 & 2 \end{bmatrix} \\ B = \begin{bmatrix} 1 & 0 & 0 & 0 \\ 0 & 1 & 0 & 0 \\ 0 & 0 & 0 & 0 \\ 0 & 0 & 0 & 0 \end{bmatrix}, \quad \mathcal{L}(G) = \begin{bmatrix} 2 & -1 & -1 & 0 \\ -1 & 3 & -1 & -1 \\ -1 & -1 & 3 & -1 \\ 0 & -1 & -1 & 2 \end{bmatrix} \\ \bar{R} = \begin{bmatrix} N_1 - N_L & E_1 - E_L & 0 & 0 & 0 & 0 & 0 & 0 \\ 0 & 0 & N_2 - N_L & E_2 - E_L & 0 & 0 & 0 & 0 \\ N_1 - N_2 & E_1 - E_2 & N_2 - N_1 & E_2 - E_1 & 0 & 0 & 0 & 0 \\ N_1 - N_3 & E_1 - E_3 & 0 & 0 & N_3 - N_1 & E_3 - E_1 & 0 & 0 \\ 0 & 0 & N_2 - N_3 & E_2 - E_3 & N_3 - N_2 & E_3 - E_2 & 0 & 0 \\ 0 & 0 & 0 & N_2 - N_4 & E_2 - E_4 & 0 & 0 & N_4 - N_2 & E_4 - E_2 \\ 0 & 0 & 0 & 0 & 0 & N_3 - N_4 & E_3 - E_4 & N_4 - N_3 & E_4 - E_3 \end{bmatrix}$$

The gains for the estimator, control laws and differentiator are  $k_1 = 30$ ,  $k_2 = 4$ ,  $k_3 = 0.3$ ,  $k_4 = 70$ ,  $k_5 = 1$  and  $k_6 = 2$ , respectively. The trajectories followed by the agents are

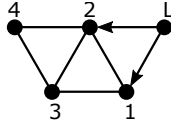


Fig. 2. Formation and communications graph.

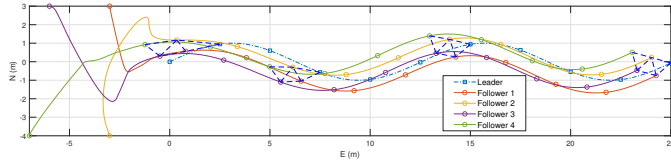


Fig. 3. Wheeled mobile robots trajectories.

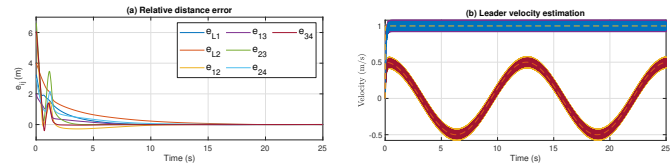


Fig. 4. (a) Inter-agent distance errors and (b) Leader velocity estimation  $\hat{v}_i$ .

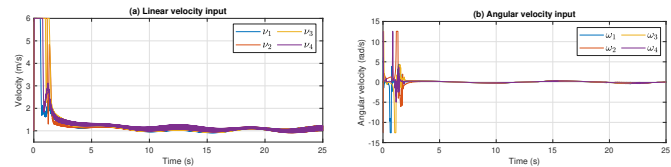


Fig. 5. (a) Control inputs  $v_i$  and (b)  $\omega_i$ .

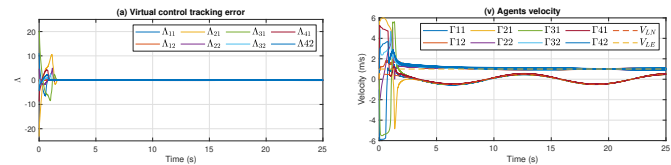


Fig. 6. (a) Virtual control tracking error  $\Lambda$  and (b) Agents velocity components  $\Gamma$ .

shown in Fig. 3, the dashed line shows the connections between agents at  $t = 2.5s$ ,  $t = 7.5s$ ,  $t = 15s$  and  $t = 25s$ , when the formation maneuver is achieved. In Fig. 4a convergence of the inter-agent distance error to zero is shown. Fig. 4b shows convergence of the estimated Leader velocity (dashed line). Fig. 5a and Fig. 5b show the control inputs  $v_i$  and  $\omega$ . Fig. 6b illustrates velocity matching.

## 6. CONCLUSIONS

In this paper, the finite-time rigidity-based formation maneuvering problem for non-holonomic agents with differential wheeled robot dynamic model was considered for the agents. A finite-time distributed leader velocity estimator was employed and finite-time distributed distance-based control laws were developed following the backstepping methodology, for these a reduced rigidity matrix  $\tilde{R}$  was proposed to allow the leader's neighbors to keep their relative distance, since the leader is a non-controlled agent and the conventional rigidity matrix involves all the agents in the system. Simulations are provided to show the ef-

fectiveness of the algorithms and prove they are able to achieve the desired objectives.

## ACKNOWLEDGEMENTS

P. Hernández-León gratefully acknowledges the financial support from CINVSTAV (SANAS-CN-2020-181) and CONACYT scholarship (CVU: 855983). J. Dávila gratefully acknowledges the financial support from SIP-IPN under grant 20200733.

## REFERENCES

- Chu, X., Peng, Z., Wen, G., and Rahmani, A. (2017). Decentralised consensus-based formation tracking of multiple differential drive robots. *International Journal of Control*, 90(11), 2461–2470.
- Ding, Z. (2013). *Nonlinear and adaptive control systems*. Control, Robotics & Sensors. Institution of Engineering and Technology.
- Hendrickx, J., Fidan, B., Changbin Yu, Anderson, B., and Blondel, V. (2008). Formation reorganization by primitive operations on directed graphs. *IEEE Transactions on Automatic Control*, 53(4), 968–979.
- Hu, J. and Hong, Y. (2007). Leader-following coordination of multi-agent systems with coupling time delays. *Physica A: Statistical Mechanics and its Applications*, 374(2), 853–863.
- Hua, Y., Dong, X., Han, L., Li, Q., and Ren, Z. (2018). Finite-time time-varying formation tracking for high-order multiagent systems with mismatched disturbances. *IEEE Transactions on Systems, Man, and Cybernetics: Systems*, Unpublished, 1–9.
- Izestiev, I. (2009). Infinitesimal rigidity of frameworks and surfaces. *Lectures on Infinitesimal Rigidity*, Kyushu University, Japan.
- Jackson, B. (2007). Notes on the rigidity of graphs. *Proc. Leivco Conf. Notes*.
- Khalil, H. (2014). *Nonlinear control*. Always Learning. Pearson Education Limited.
- Levant, A. (2003). Higher-order sliding modes, differentiation and output-feedback control. *International Journal of Control*, 76(9-10), 924–941.
- Mehdifar, F., Hashemzadeh, F., Baradarannia, M., and de Queiroz, M. (2018). Finite-Time rigidity-based formation maneuvering of multiagent systems using distributed finite-time velocity estimators. *IEEE Transactions on Cybernetics*, 49(12), 4473–4484.
- Mesbahi, M. and Egerstedt, M. (2010). *Graph theoretic methods in multiagent networks*. Princeton Univ Press.
- Oh, K.K., Park, M.C., and Ahn, H.S. (2015). A survey of multi-agent formation control. *Automatica*, 53, 424–440.
- Peng, Z., Wen, G., Rahmani, A., and Yu, Y. (2015). Distributed consensus-based formation control for multiple nonholonomic mobile robots with a specified reference trajectory. *International Journal of Systems Science*, 46(8), 1447–1457.
- Shtessel, Y., Edwards, C., Fridman, L., and Levant, A. (2014). *Sliding mode control and observation*. Springer.
- Wang, Y., Li, T., and Philip Chen, C.L. (2017). Adaptive terminal sliding mode control for formations of underactuated vessels. In F. Sun, H. Liu, and D. Hu (eds.), *Cognitive Systems and Signal Processing*, 27–35. Springer Singapore, Singapore.